RNA-Puzzles: A CASP-like evaluation of RNA three-dimensional structure prediction

JOSÉ ALMEIDA CRUZ,[1] MARC-FRÉDÉRICK BLANCHET,[2] MICHAL BONIECKI,[3] JANUSZ M. BUJNICKI,[3,4] SHI-JIE CHEN,[5] SONG CAO,[5] RHIJU DAS,[6,7] FENG DING,[8] NIKOLAY V. DOKHOLYAN,[8] SAMUEL COULBOURN FLORES,[9] LILI HUANG,[10] CHRISTOPHER A. LAVENDER,[11] VÉRONIQUE LISI,[2] FRANÇOIS MAJOR,[2] KATARZYNA MIKOLAJCZAK,[3] DINSHAW J. PATEL,[10] ANNA PHILIPS,[3,4] TOMASZ PUTON,[4] JOHN SANTALUCIA,[12,13] FREDRICK SIJENYI,[13] THOMAS HERMANN,[14] KRISTIAN ROTHER,[4] MAGDALENA ROTHER,[4] ALEXANDER SERGANOV,[10] MARCIN SKORUPSKI,[4] TOMASZ SOLTYSINSKI,[3] PARIN SRIPAKDEEVONG,[6,7] IRINA TUSZYNSKA,[3] KEVIN M. WEEKS,[11] CHRISTINA WALDSICH,[15] MICHAEL WILDAUER,[15] NEOCLES B. LEONTIS,[16] and ERIC WESTHOF[1,17]

[1]Architecture et Réactivité de l'ARN, Université de Strasbourg, IBMC-CNRS, F-67084 Strasbourg, France
[2]Institute for Research in Immunology and Cancer (IRIC), Department of Computer Science and Operations Research, Université de Montréal, Montréal, Québec H3C 3J7, Canada
[3]Laboratory of Bioinformatics and Protein Engineering, International Institute of Molecular and Cell Biology in Warsaw, 02-109 Warsaw, Poland
[4]Laboratory of Bioinformatics, Institute of Molecular Biology and Biotechnology, Faculty of Biology, Adam Mickiewicz University, 61-614 Poznan, Poland
[5]Department of Physics and Department of Biochemistry, University of Missouri, Columbia, Missouri 65211, USA
[6]Department of Biochemistry, [7]Department of Physics, Stanford University, Stanford, California 94305, USA
[8]Department of Biochemistry and Biophysics, University of North Carolina, School of Medicine, Chapel Hill, North Carolina 27599, USA
[9]Computational & Systems Biology Program, Institute for Cell and Molecular Biology, Uppsala University, 751 05 Uppsala, Sweden
[10]Structural Biology Program, Memorial Sloan-Kettering Cancer Center, New York, New York 10021, USA
[11]Department of Chemistry, University of North Carolina, Chapel Hill, North Carolina 27599, USA
[12]Department of Chemistry, Wayne State University, Detroit, Michigan 48202, USA
[13]DNA Software, Ann Arbor, Michigan 48104, USA
[14]Department of Chemistry and Biochemistry, University of California at San Diego, La Jolla, California 92093, USA
[15]Max F. Perutz Laboratories, Department of Biochemistry, University of Vienna, Vienna 1030, Austria
[16]Department of Chemistry and Center for Biomolecular Sciences, Bowling Green State University, Bowling Green, Ohio 43403, USA

ABSTRACT

We report the results of a first, collective, blind experiment in RNA three-dimensional (3D) structure prediction, encompassing three prediction puzzles. The goals are to assess the leading edge of RNA structure prediction techniques; compare existing methods and tools; and evaluate their relative strengths, weaknesses, and limitations in terms of sequence length and structural complexity. The results should give potential users insight into the suitability of available methods for different applications and facilitate efforts in the RNA structure prediction community in ongoing efforts to improve prediction tools. We also report the creation of an automated evaluation pipeline to facilitate the analysis of future RNA structure prediction exercises.

Keywords: 3D prediction; bioinformatics; force fields; structure

INTRODUCTION

The determination of the atomic structure of any biological macromolecule, RNA molecules being no exception, contributes regularly toward the understanding of the molecular

[17]Corresponding author.
E-mail E.Westhof@ibmc-cnrs.unistra.fr.

basis of the underlying biological process. Each of the current experimental methods for determining the three-dimensional (3D) structures of RNA molecules—X-ray crystallography, NMR, and cryo-electron microscopy—requires great expertise and substantial technical resources. Therefore, the ability to reliably predict accurate RNA 3D structures based solely on their sequences, or in concert with efficiently obtained biochemical information, is an important problem and constitutes a major intellectual challenge (Tinoco and Bustamante 1999). Recent decades have seen several

significant theoretical advances toward this goal that include:

1. The development of predictive models for RNA secondary structure, pioneered by the seminal work of Tinoco and coworkers (Tinoco et al. 1973) and made commonly available in a number of tools that perform reasonably well for sequences of moderate size (Hofacker et al. 1994; Zuker 2003; Reuter and Mathews 2010);
2. The ability to meaningfully deduce RNA structures through comparative sequence analysis (Woese et al. 1980; Michel and Westhof 1990);
3. The systematization of the knowledge about RNA architecture and interactions (Leontis and Westhof 2001) to gain a handle on the rapid increase in the number and size of RNA molecules with published structures available in public databases (Berman et al. 2000);
4. The availability of comprehensive sequence alignments (Gardner et al. 2009) permitting the study of the relationship between structure and sequence;
5. The development of improved molecular dynamics force fields and techniques (Ditzler et al. 2010);
6. Finally, the increasing availability of inexpensive computing power and data storage allows for extensive computational searches.

As a consequence, exciting developments in the field of de novo structure prediction have occurred in the last few years: computer-assisted modeling tools (Martinez et al. 2008; Jossinet et al. 2010); conformational space search (Parisien and Major 2008); discrete molecular dynamics (Ding et al. 2008a); knowledge-based, coarse-grained refinement (Jonikas et al. 2009); template-based (Flores and Altman 2010; Rother et al. 2011b); and force-field-based approaches (Das et al. 2010) inspired by proven protein-folding techniques adapted to the RNA field (for review, see Rother et al. 2011a). All these new approaches are pushing the limits of automatic RNA structure prediction from short sequences of a few nucleotides to medium-sized molecules with several dozens. Assuming continuing, steady progress, one can expect that in the near-to-medium future, de novo prediction of RNA 3D structures will become as common and useful as RNA secondary structure prediction is today.

These promising results and the increasing number of available tools raise the need for objective evaluation and comparison. Indeed, the establishment of a benchmark for RNA structure prediction has become essential in order to optimize and improve the current methods and tools for structural prediction. Here, we present the results of a blind exercise in RNA structure prediction. Sequences of RNA structures solved by crystallographers were provided, before publication, to active research groups that develop new methods and perform RNA 3D structure prediction. Comparisons between predicted and experimental X-ray struc-tures were undertaken once the structures were published. The resulting benchmarks function as a snapshot of the current status of this field. On the basis of this successful first round, we would like to extend to RNA the idea established by the protein structure prediction community (Moult 2006) and to propose a continuous, open, and collective structure prediction experiment, with the essential, active participation of experimentalists.

RNA-PUZZLES

RNA-Puzzles is a collective blind experiment for evaluation of de novo RNA structure prediction. With this initiative, we hope to (1) assess the cutting edge of RNA structure prediction techniques; (2) compare the different methods and tools, elucidating their relative strengths and weaknesses and clarifying their limits in terms of sequence length and structure complexity; (3) determine what has still to be done to achieve an ultimate solution to the structure prediction problem; (4) promote the available methods and guide potential users in the choice of suitable tools for different problems; and (5) encourage the RNA structure prediction community in their efforts to improve the current tools.

The procedure that governs *RNA-Puzzles* is straightfor-ward. Based on the successful first round, we propose the following steps:

- Complete nucleotide sequences will be periodically released to interested groups who agree to keep sequence information confidential. These target sequences corre-spond to experimentally determined crystallographic or NMR structures, kindly provided by experimental groups, and not yet published in any form. Confidentiality of RNA sequence information is essential to protect the target selection and molecular engineering strategies of par-ticipating experimental groups.
- The interested groups will have a specified length of time (usually 4–6 wk) to submit their predicted models to a website in a standard pdb format that respects atom naming and nomenclature conventions.
- The predicted models will be evaluated with regard to stereochemical correctness, topology, and geometrical similarity, relative to the experimental structure.
- After publication of the original experimental structures, all predicted models, experimental results, and compar-ative data will be made publicly available.

To set up and automate these steps, the *RNA-Puzzles* team has put together a public website for announcing new experiments and publishing results of completed experiments. The website also provides a processing pipeline to carry out model evaluation. The *RNA-Puzzles* site is publicly available at http://paradise-ibmc.u-strasbg.fr/rnapuzzles/.

STRUCTURE ANALYSIS AND COMPARISON

The evaluation of the biological value of a structural model raises many questions. How do you determine if a given model is a meaningful prediction? What is, in fact, a biologically meaningful prediction? Which questions should a structural model answer? Clearly, addressing some questions requires very high precision (1–2 Å or below); whereas, in other cases, important insights may be obtained with residue-level or domain-level precision.

To evaluate the predictive success of the proposed models, we established two general criteria:

1. The predicted model must be geometrically and topologically as close as possible to the experimentally determined structure, used as the reference. It is assumed that the crystal structure or NMR structure is correct within the limitations of the experimental methods.
2. The predicted model must be stereochemically correct (with bond distances and intermolecular contacts close to the experimentally observed values).

To geometrically compare predicted models with the experimental structures, we used the Root Mean Square Deviation (RMSD) measure and the Deformation Index (DI) (Parisien et al. 2009). The RMSD is the usual measure of distance between two superimposed structures defined by the formula:

$$RMSD(A, B) = \sqrt{\frac{\sum\limits_{i=1}^{n} (a_i - b_i)^2}{n}},$$

in which A and B are the modeled and experimental structures and $(a_i - b_i)$ represents the distance between the *i*-th atoms of the two structures. The DI is given by:

$$DI(A, B) = \frac{RMSD(A, B)}{MCC(A, B)},$$

in which MCC is the Matthews Correlation Coefficient (Matthews 1975) computed on the individual base-pair and base-stacking predictions. The reason for this choice is that the RMSD, as a measure of similarity, does not account for specific RNA features such as the correctness of base-pair and stacking interactions. The DI score complements the RMSD values by introducing those specific features in the metric. Using the DI value, the quality of two models with close RMSDs can be discriminated according to the accuracy of their predictions of the base-pairing and stacking interactions of the experimental structure. As we observed in the first experiments, the ranking of the models is sensitive to the chosen metric (see Tables 1–3). Such observations were also made during the CASP competitions of protein structure prediction (see Marti-Renom et al. 2002). Use of diverse, complementary metrics should contribute to the design of improved metrics and an understanding of their relative strengths and limitations.

In a recent work (Hajdin et al. 2010), Weeks, Dokholyan, and coworkers showed that when sampling the conformational space of an RNA molecule using discrete molecular dynamics, the RMSD values are distributed normally with a mean related to the length of the molecule by the power law:

$$< RMSD > = a \times N^{0.41} - b$$

Here, N is the number of nucleotides, and a and b are constants that depend on whether secondary structure information is provided as input to the molecular dynamic simulation. From this observation, it is possible to compute the significance level (P-value) of a prediction with a given RMSD with respect to an accepted structure. This P-value corresponds to the probability that a given structure prediction is better than that expected by chance (Hajdin et al. 2010). Structure models with P-values <0.01 represent, in general, successful predictions of a global RNA fold. The P-value is sensitive to the amount of preexisting information available for a given structure prediction problem, especially whether the pattern of base-pairing is known in advance. For most structure prediction problems, much or all of the secondary structure is known and is used as a constraint during structure prediction and refinement. In this round of *RNA-Puzzles*, P-value analysis was appropriate for Puzzle 3 (below).

The stereochemical correctness of the predicted models was evaluated with MolProbity (Davis et al. 2007), which provides quality validation for 3D structures of nucleic acids. MolProbity performs several automatic analyses, from checking the lengths of H-bonds present in the model to validating the compliance with the rotameric nature of the RNA backbone (Murray et al. 2003). The reduce-build script of MolProbity was used for adding hydrogen atoms to the heavy atoms of the models. As a single measure of stereochemical correctness, we chose the *clash score*, i.e., the number of steric clashes per thousand residues (Word et al. 1999).

All of the computed values are shown in a comparison summary page, which ranks the submitted models according to each of the computed metrics. In addition to the comparison summary, we provide a report for each of the predicted models. The report presents the structural superposition between predicted model and experimental structure, the analysis of the predicted base pairs—correctly predicted (true positives), incorrectly predicted (false positives), and missed (false negatives)—and a complete Deformation Profile matrix (DP) (Parisien et al. 2009), which provides an evaluation of the predictive quality of a model at multiple scales.

THE PROBLEMS

Two crystallography laboratories sent coordinates for the prediction contest: the laboratories of Thomas Hermann at UC San Diego and of Dinshaw Patel and Alexander Serganov at the Memorial Sloan-Kettering Cancer Center. The three trial experiments were the following.

Problem 1: Dimer

Predict the structure of the following sequence:

$$5'\text{-}CCGCCGCGCCAUGCCUGUGGCGG\text{-}3',$$

knowing that the crystal structure shows a homodimer that contains two strands of the sequence that hybridize with blunt ends (C-G closing base pairs). The solution structure corresponds to the regulatory element from human thymidylate synthase mRNA (Dibrov et al. 2011a), which, in the crystal, forms a dimer with two asymmetrical internal loops, despite perfect sequence symmetry (Fig. 1A,B). The crystal structure was resolved to 1.97 Å resolution. A total of 14 predicted models were submitted with an RMSD ranging from 3.41 Å to 6.94 Å (mean RMSD of 4.7 Å) (Table 1).
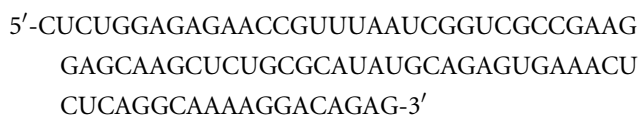
Problem 2: Square

The crystal structure, which was resolved to 2.2 Å resolution, shows a 100-nt square of double-stranded RNA that self-assembles from four identical inner and four identical outer strands (Dibrov et al. 2011b). The secondary structure

shown was used for the design of the square. Actual base-pairing in the crystal may deviate. 3D coordinates of the nucleotides in the inner strands (B, D, F, H) were provided. What are the structures of the outer strands (A, C, E, G)?

The square is formed by four helices connected by four single-stranded loops. All of the helices are identical at the sequence level, and so are all the loops (Fig. 2).

Problem 3: A riboswitch domain

A riboswitch domain was crystallized. The sequence is the following:

$$5'\text{-CUCUGGAGAGAACCGUUUAAUCGGUCGCCGAAG}$$
$$GAGCAAGCUCUGCGCAUAUGCAGAGUGAAACU$$
$$CUCAGGCAAAAGGACAGAG\text{-}3'$$

The crystallized sequence was slightly different (an apical loop was replaced by a GAAA loop), but this detail of RNA crystal engineering was not disclosed to modelers to protect the crystallographers (Fig. 3A,B; Huang et al. 2010).

RESULTS

Eight research groups participated in the *RNA-Puzzles* experiments. The Bujnicki group used a hybrid strategy previously developed for protein modeling in the course of the CASP experiment (Kosinski et al. 2003). The Chen lab used a multi-scale, free energy landscape–based RNA folding model (Vfold model) (Chen 2008; Cao and Chen 2011). The Das group used the stepwise assembly (SWA) method for
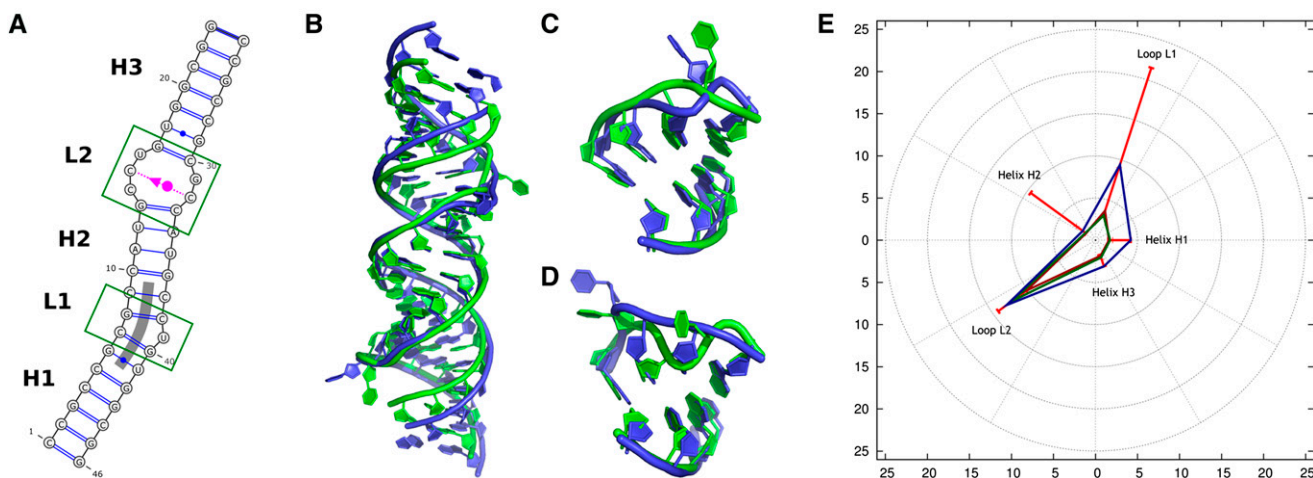

FIGURE 1. Problem 1—An RNA dimer. (*A*) Secondary structure of the reference RNA molecule. Note that the structure is symmetric on the sequence level but is asymmetric in the crystal, indicating that crystal-packing forces played a significant role in the conformation of this RNA. The interaction (in magenta) was detected with the RNAView (Yang et al. 2003) annotation program but not with MC-Annotated (Gendron et al. 2001). (Thick gray band) Coaxial stacking between helices. X-ray structures of the reference RNA molecule (green) and the lowest RMSD predicted models (blue) for the complete Das model 3 (*B*), details of loop L1 of Das model 1 (*C*), and details of loop L2 of Das model 3 (*D*). (*E*) Deformation Profile values for each of the five domains of the homodimer. (Colored lines) The DP values for the two predicted models with lowest RMSD, Das model 3 (dark red), and Das model 1 (dark green), and for the predicted model with highest RMSD, Dokholyan model 1 (dark blue). (Radial red lines) The minimum, maximum, and mean DP values for each domain.

TABLE 1. Summary of the results for Puzzle 1

Problem 1 Group[a]	Number[b]	RMSD[c]	Rank[d]	DI all[e]	Rank[d]	INF all[f]	Rank[d]	INF wc[g]	Rank[d]	INF stack[h]	Rank[d]	Clash Score[i]	Rank[d]	L1[j]
Das	3	3.41	1	3.66	1	0.93	1	0.95	2	0.92	1	0.00	5	x
Das	1	3.58	2	3.89	2	0.92	3	0.95	1	0.91	2	0.00	3	x
Das	4	3.91	3	4.31	3	0.91	4	0.91	8	0.91	4	0.00	4	
Major	1	4.06	4	4.57	4	0.89	5	0.95	6	0.87	5	66.40	11	
Chen	1	4.11	5	5.01	6	0.82	9	0.87	11	0.80	8	0.68	6	
Das	2	4.34	6	4.70	5	0.92	2	0.95	4	0.91	3	1.36	7	x
Das	5	4.56	7	5.36	7	0.85	7	0.88	10	0.84	7	0.00	2	
Bujnicki	3	4.66	8	5.75	9	0.81	11	0.95	3	0.74	14	54.73	10	x
Bujnicki	4	4.74	9	6.59	11	0.72	14	0.65	14	0.75	13	83.33	14	
Bujnicki	5	4.89	10	6.26	10	0.78	13	0.78	13	0.80	9	81.98	13	
Bujnicki	1	5.07	11	5.75	8	0.88	6	0.93	7	0.86	6	0.00	1	x
Bujnicki	2	5.43	12	6.75	12	0.80	12	0.90	9	0.77	12	71.57	12	x
Santalucia	1	5.69	13	6.75	13	0.84	8	0.95	5	0.79	11	39.86	9	
Dokholyan	1	6.94	14	8.55	14	0.81	10	0.86	12	0.79	10	31.74	8	
Mean		4.67		5.56		0.85		0.89		0.83				
Standard deviation		0.93		1.34		0.06	N	0.09		0.07				
										X-Ray Model		1.35		

Values in each row correspond to a predicted model.
[a]Name of the research group that submitted the model.
[b]Number of the model among all models from the same group.
[c]RMSD of the model compared with the accepted structure.
[d]Columns indicate the rank of the model with respect to the left-hand column metric.
[e]DI_{all} is the Deformation Index taking into account all interactions (stacking, Watson-Crick, and non-Watson-Crick).
[f]INF_{all} is the Interaction Network Fidelity taking into account all interactions.
[g]INF_{wc} is the Interaction Network Fidelity taking into account only Watson-Crick interactions.
[h]INF_{stack} is the Interaction Network Fidelity taking into account only stacking interactions.
[i]Clash Score as computed by the MolProbity suite (Davis et al. 2007).
[j]An "x" in this column indicates models that correctly predict base-pair interactions in loop L1. No model correctly predicted all interactions in loop L2.

recursively constructing atomic-detail biomolecular structures in small building steps (Sripakdeevong et al. 2011). The Dokholyan group adopted a multi-scale molecular dynamics approach (Ding and Dokholyan 2012). The Flores group used the RNABuilder program, a computer-assisted RNA modeling tool (Flores and Altman 2010). The Major group applied the fully automated MC-Fold and MC-Sym pipeline they developed (Parisien and Major 2008). The Santalucia group also applied their own program.

The amount of time required to produce the models and the degree of automation varied as a function of approach. One point should be emphasized. Compared with CASP protein targets, an RNA puzzle typically involves multiple "mini-puzzles" such as separate tertiary modules and specific non-Watson-Crick pairs. There are several examples of this from this first round, for example, the four corners and the four helices of the nanosquare. Thus, a single RNA puzzle can provide multiple challenges for testing modeling methods.

Problem 1: Dimer

Fourteen predicted models were submitted. The RMSDs range from 3.41 Å to 6.94 Å (with a mean of 4.67 Å). The base-pair interactions were correctly predicted in almost all

models with >85% of WC base pairs correctly predicted in all but two models and >75% of stacking interaction predicted in all but one model. Contrary to the X-ray structure, most of the proposed models present a symmetric structure. The only exceptions were the models from the Das laboratory (see Table 1). From the analysis of the Deformation Profile values (Fig. 1E), it is clear that the internal loops were the domains most difficult to predict (Fig. 1C,D) and that helix H2, probably because of its location between the loops, presents a particularly large interval of DP values. Several models present high values for the Clash Score, which could reflect the need for updated dictionaries of distances and angles or stronger constraints toward the dictionary values.

Problem 2: Square

Thirteen predicted models were submitted with RMSDs ranging from 2.3 Å to 3.65 Å (mean RMSD of 2.9 Å) (see Table 2). The RMSDs of solutions to this problem are the lowest of all three problems, which is expected because one-half of each base pair was provided in the initial puzzle description. As expected, the helical regions are better predicted than loops, with mean DP values between 5 and 10 for all loops and <5 for three of the helices (Fig. 2C–E),
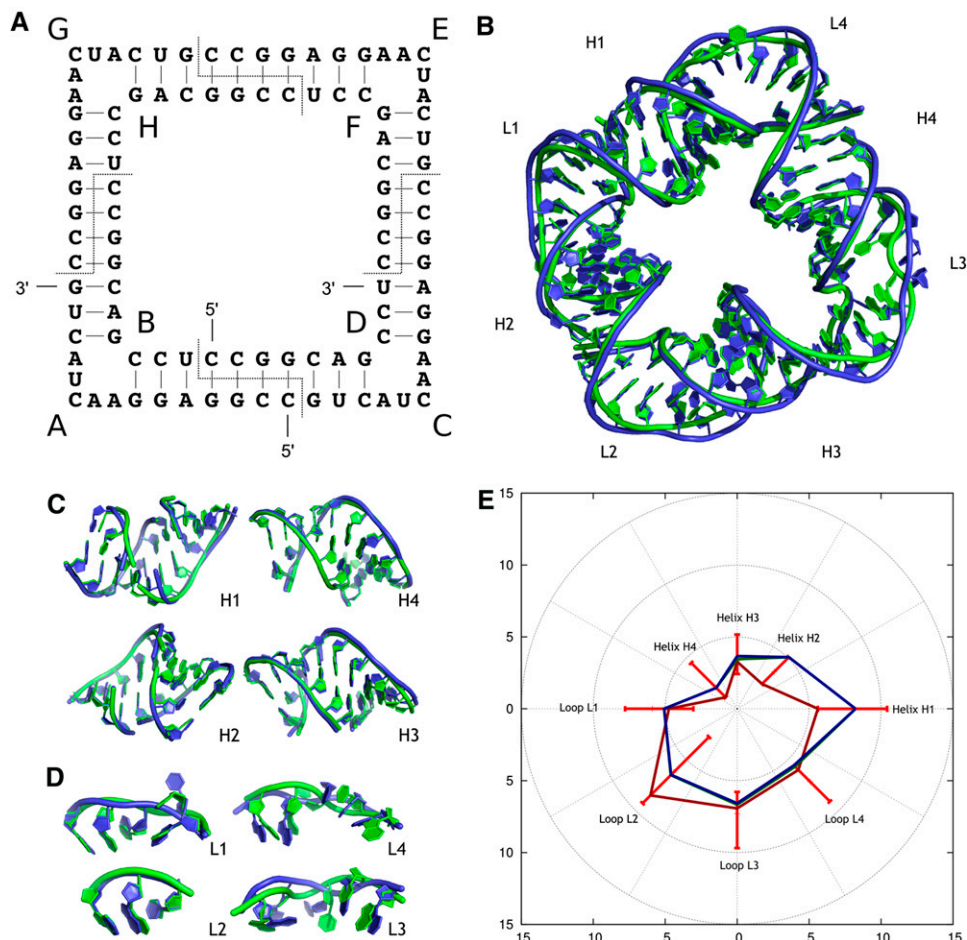
FIGURE 2. Problem 2—An RNA square. (*A*) Secondary structure of the reference RNA molecule. X-ray structures of the reference RNA molecules (green) and the predicted models with lowest RMSDs (blue) for the full molecule and Bujnicki model 2 (*B*); details of helices H1, H2, and H4 of Das model 1 and helix H3 of Bujnicki model 2 (*C*); and details of loops L1 and L2 of Santalucia model 1, loop L3 of Dokholyan model 1, and loop L4 of Bujnicki model 3 (*D*). (*E*) Deformation Profile values for the three predicted models with lowest RMSD: Bujnicki model 2 (dark red), Bujnicki model 3 (dark green), and Das model 1 (dark blue). (Radial red lines) The minimum, maximum, and mean DP values for each domain.

with the exception of helix 1, in which the three base pairs close to loop 4 deviate slightly from the canonical Watson-Crick geometry. As for Problem 1, the base-pairing and stacking were generally well predicted, but, again, there are a couple of very high Clash Scores values, with most models giving values below that of the X-ray structure.

Problem 3: A riboswitch domain

This problem posed the most intricate tertiary structure and was the most complex to model. Twelve predicted models were submitted with RMSDs ranging from 7.24 Å to 22.99 Å (mean RMSD of 14.4 Å) (Table 3). The *P*-values are correspondingly high (except maybe for the first model). The overall molecular architecture was reasonably well predicted by the two models with the lowest RMSD values. The interdomain DP values for the 10 pairwise helix–helix predictions (Fig. 3D) show that the Chen model presents

the lowest DP for the three-way junction (P1–P2, P1–P3, and P2–P3) and a consistently lower than average DP for the coaxial stacking of P2–P3–P3a–P3b. This coaxial stacking was also predicted reasonably well (DP < 15) by five of the models (Table 4). Finally, the ligand-binding cleft active site, corresponding in a 13-nt internal loop between domains P3 and P3a, was predicted with an RMSD < 6 Å in all models except one (Fig. 3C; Table 5). Non-Watson-Crick base pairs, however, were not well predicted.

DISCUSSION

Here we have presented *RNA-Puzzles*, a collective blind experiment for de novo RNA structure prediction evaluation. We hope that this initiative will function as an open forum where members of the RNA modeling community can compare their methods, tools, and results and where newcomers to the field can get a head start. The success of
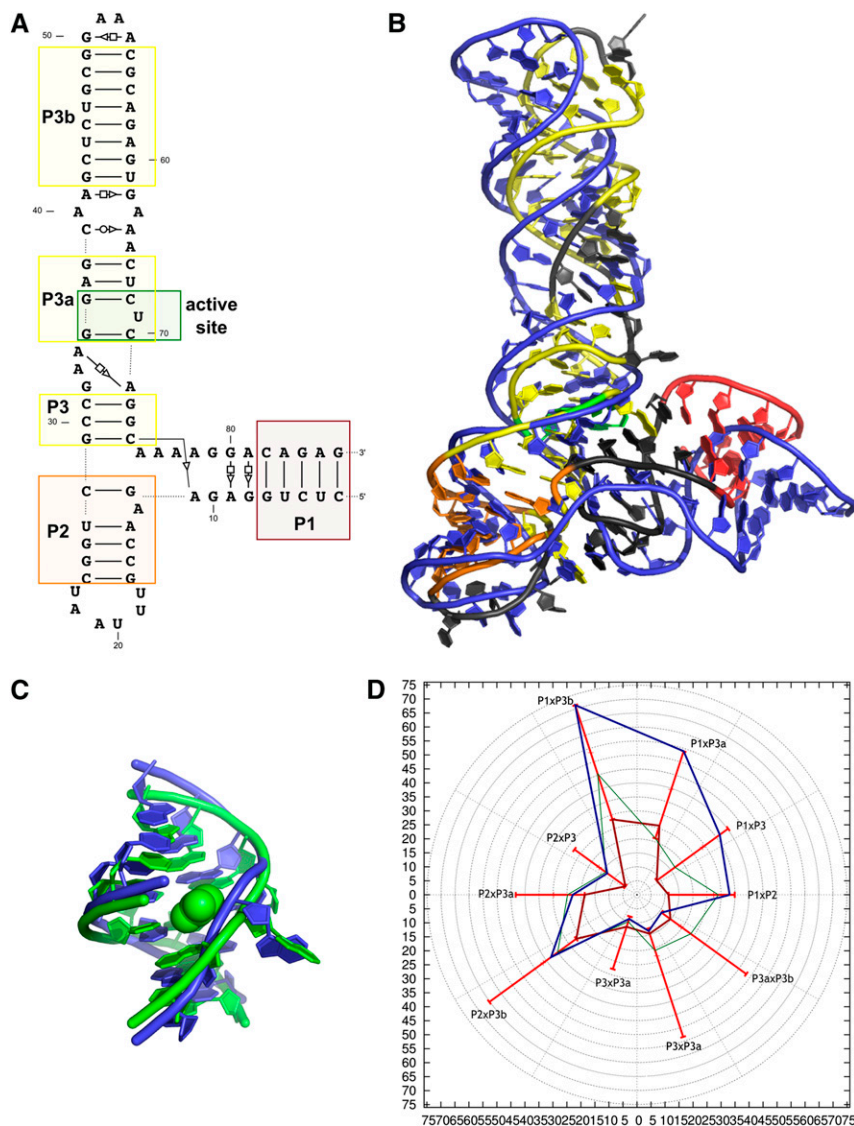
FIGURE 3. Problem 3—A riboswitch domain. (*A*) Secondary structure of the reference RNA molecule. (*B*) X-ray structure of the reference RNA molecule (P1 [red]; P2 [orange]; P3, P3a, P3b [yellow]; active site [green]) and the predicted model of the lowest RMSD Chen model 1 (blue). (*C*) Detail of the ligand binding pocket for the X-ray structure (green) and the lowest RMSD Chen model 1 (blue). (*D*) Deformation Profile values of the pairwise helical interdomain regions (P1, P2, P3, P3a, and P3b) for the three models with lowest RMSDs: Chen model 1 (dark red), Dokholyan model 2 (dark green), and Das model 5 (dark blue). (Radial red lines) The minimum, maximum, and mean DP values for each interdomain pair.

compactly encoded in the B-factor field of PDB atom records. The number of submissions should be limited and multiple submissions ranked by the authors. (2) In addition, it will be worthwhile to improve model scoring and ranking so as to produce an absolute ranking of all models, taking into account local and global model quality. (3) Because the RNA structure database continues to grow, template-based methods are becoming increasingly important, and, consequently, future RNA puzzles should also include structures of homologs of existing folds (for example, a riboswitch with an alternative ligand or mutation). (4) Finally, we plan to extend the contest to include structures of RNA–protein complexes.

The assessment of model accuracy requires reliable and meaningful metrics for comparisons between the models and the experimentally determined structures used as the accepted structure. In addition to the metrics currently used (generic to all macromolecules or specific for RNA), it may be worthwhile to include metrics that have been shown to perform very well at both global and local levels for assessing the very wide range of model qualities (from very inaccurate to very accurate) (Zemla 2003; Zhang and Skolnick 2004), as have been generally accepted in the protein structure prediction field and are used by assessors in the CASP challenges. We are hopeful that, with extensive community support, this round of *RNA-Puzzles* is the first of what will become a vigorous and ongoing discussion of the frontiers of RNA structure prediction and refinement.

RNA-Puzzles will depend critically on engagement by the prediction community and the generosity of the experimental community. Most importantly, this work will, hopefully, convince additional structural biology groups to offer problems to the modeling community in the future.

This first contest had clear limitations, and several improvements have already been planned. (1) As established for CASP, in the future, modelers will be asked to predict the deviations of their own models from the unknown native structure, at the level of individual residues or atoms (in angstroms). These values could, for example, be

MATERIALS AND METHODS

The following provides a brief description of the methodology used by the modeling groups, together with comments.

Bujnicki group

The Bujnicki group used a hybrid strategy previously developed for protein modeling in the course of the CASP experiment (Kosinski et al. 2003). Briefly, initial models were constructed by template-based modeling and fragment assembly, with constraints on secondary structure, using the comparative RNA modeling tool ModeRNA (Rother et al. 2011b). For RNA Puzzle Problem 2, the secondary

TABLE 2. Summary of the results for Puzzle 2

Problem 2

Group[a]	Number[b]	RMSD[c]	Rank[d]	DI all[e]	Rank[d]	INF all[f]	Rank[d]	INF wc[g]	Rank[d]	INF nwc[h]	Rank[d]	INF stack[i]	Rank[d]	Clash Score[j]	Rank[d]
Bujnicki	2	2.3	1	2.83	1	0.81	8	0.92	9	0	13	0.79	7	14.54	2
Bujnicki	3	2.33	2	2.9	3	0.8	10	0.91	10	0	2	0.77	9	0.62	1
Das	1	2.5	3	2.9	2	0.86	2	0.96	5	0	8	0.85	2	19.8	5
Dokholyan	1	2.54	4	3.09	5	0.82	6	0.9	11	0	1	0.8	5	19.85	6
Bujnicki	1	2.65	5	2.99	4	0.89	1	0.96	4	0	3	0.86	1	15.47	3
Chen	1	2.83	6	3.74	9	0.76	13	0.9	12	0	9	0.69	13	18.66	4
Das	4	2.83	7	3.46	6	0.82	7	0.97	3	0	12	0.78	8	23.82	8
Major	1	2.98	8	3.82	10	0.78	12	0.95	7	0	10	0.71	12	134.26	12
Das	3	3.03	9	3.67	7	0.83	5	0.97	1	0	6	0.8	6	25.37	10
Das	2	3.05	10	3.69	8	0.83	4	0.97	2	0	7	0.81	3	23.51	7
Das	5	3.46	11	4.18	11	0.83	3	0.96	6	0	11	0.81	4	24.75	9
Flores	1	3.48	12	4.4	12	0.79	11	0.89	13	0	5	0.77	10	165.57	13
Santalucia	1	3.65	13	4.54	13	0.81	9	0.92	8	0	4	0.75	11	25.73	11
Mean		2.90		3.55		0.82		0.94		0.00		0.78			
Standard deviation		0.44		0.59		0.03		0.03		0.00		0.05			
												X-Ray Model		36.10	

Values in each row correspond to a predicted model.
[a]Name of the research group that submitted the model.
[b]Number of the model among all models from the same group.
[c]RMSD of the model compared with the accepted structure.
[d]Columns indicate the rank of the model with respect to the left-hand column metric.
[e]DI$_{all}$ is the Deformation Index taking into account all interactions (stacking, Watson-Crick, and non-Watson-Crick).
[f]INF$_{all}$ is the Interaction Network Fidelity taking into account all interactions.
[g]INF$_{wc}$ is the Interaction Network Fidelity taking into account only Watson-Crick interactions.
[h]INF$_{nwc}$ is the Interaction Network Fidelity taking into account only non-Watson-Crick interactions.
[i]INF$_{stack}$ is the Interaction Network Fidelity taking into account only stacking interactions.
[j]Clash Score as computed by the MolProbity suite (Davis et al. 2007).

structure was provided by the organizers, while for Problem 3, it was calculated as a consensus of more than 20 methods using the RNA metaserver (http://genesilico.pl/rnametaserver/). The initial models were expected to possess approximately correct Watson-Crick base-pairing and stacking interactions within individual structural elements, but their mutual orientations and tertiary contacts required optimization.

The initial models were subjected to global refinement using SimRNA, a de novo RNA folding method (Rother et al. 2012), which was inspired by the REFINER method for protein folding (Boniecki et al. 2003). SimRNA uses a coarse-grained representation, with only three centers of interaction per nucleotide residue. The backbone is represented by atoms P of the phosphate group and C4′ of the ribose moiety, whereas the base is represented by just one nitrogen atom of the glycosidic bond (N9 for purines or N1 for pyrimidines). The remaining atoms are neglected. This simplified representation allows reproducing the main characteristics of the RNA molecule such as base-pairing and stacking, and the backbone in helix, while significantly lowering the computational cost for conformational transitions and energy calculations. As an "energy" function, SimRNA uses a statistical potential derived from frequency distributions of geometrical properties observed in experimentally determined RNA structures. Terms of the SimRNA energy function (for the virtual bond lengths, flat and torsion angles, pairwise interactions between the three atom types) were generated using reverse Boltzmann statistics. For searching the conformational space, SimRNA uses Monte Carlo dynamics controlled by an asymmetric Metropolis method (Metropolis and Ulam 1949) that accepts or rejects new conformations depending on the energy change associated with the conformational change, with the probability of acceptance depending on the temperature of the system. Simulations can be run in the isothermal or energy minimization (simulated annealing) mode, or in conformation space search mode (replica exchange). While SimRNA allows for simulations that use only the sequence information, starting from an extended structure, it can accept user-defined starting structures and restraints that specify distances or allowed distance ranges for user-defined atom pairs. For *RNA-Puzzles*, the Bujnicki group used restraints on secondary structure that allowed the predicted base pairs to be maintained. Following a series of simulations, lowest-energy structures were selected for the final refinement.

The final models were built by first reconstructing the full-atom representation using RebuildRNA (P Lukasz, M Boniecki, and JM Bujnicki, unpubl.) and then optimizing atomic detail of selected residues with SCULPT (Surles et al. 1994) and HyperChem 8.0 (Hypercube Inc.). For Problem 2, the known coordinates of four strands were used as provided by the organizers and "frozen" at the optimization stage.

The computer calculation time (on a single processor) was as follows: ModeRNA: <2 h; SimRNA and RebuildRNA: ~150 h; SCULPT <1 h; HyperChem: ~12 h.

In the case of the Bujnicki group, the ratio of human to computer time was relatively large (approximately equal), because

TABLE 3. Summary of the results for Puzzle 3

Problem 3

Group[a]	Number[b]	RMSD[c]	Rank[d]	DI all[e]	Rank[d]	INF all[f]	Rank[d]	INF wc[g]	Rank[d]	INF nwc[h]	Rank[d]	INF stack[i]	Rank[d]	Clash Score[j]	Rank[d]	P-value[k]	Rank[d]
Chen	1	7.24	1	9.84	1	0.74	2	0.86	5	0	6	0.73	1	1.1	3	2.01E-05	1
Dokholyan	2	11.46	2	16.1	2	0.71	6	0.82	9	0	9	0.71	6	41.21	10	3.90E-02	2
Das	5	11.97	3	16.42	3	0.73	5	0.9	1	0.36	5	0.71	3	1.1	4	6.92E-02	3
Bujnicki	1	12.19	4	17.49	5	0.7	7	0.82	10	0	10	0.7	7	14.72	8	8.71E-02	4
Das	2	12.2	5	16.6	4	0.74	3	0.86	6	0.4	2	0.73	2	0.74	2	8.83E-02	5
Major	2	13.7	6	23.33	10	0.59	11	0.67	11	0	8	0.61	10	93.52	12	3.03E-01	6
Bujnicki	2	14.06	7	22.51	7	0.62	10	0.83	8	0	7	0.59	11	5.15	7	3.75E-01	7
Das	1	15.48	8	20.9	6	0.74	1	0.87	4	0.57	1	0.71	5	0	1	6.81E-01	8
Dokholyan	1	15.92	9	23.28	9	0.68	9	0.9	2	0	12	0.66	9	39.37	9	7.629E-01	9
Das	3	16.95	10	23.17	8	0.73	4	0.89	3	0.4	3	0.71	4	1.47	5	9.02E-01	10
Das	4	18.3	11	26.55	11	0.69	8	0.85	7	0.38	4	0.67	8	2.21	6	9.79E-01	11
Major	1	22.99	12	45.27	12	0.51	12	0.39	12	0	11	0.59	12	75.11	11	1.00E+00	12
Mean		14.37		21.79		0.68		0.80		0.18		0.68					
Standard deviation		3.99		8.69		0.07		0.14		0.22		0.05					
												X-Ray Model		1.83			

Values in each row correspond to a predicted model.
[a]Name of the research group that submitted the model.
[b]Number of the model among all models from the same group.
[c]RMSD of the model compared with the accepted structure.
[d]Columns indicate the rank of the model with respect to the left-hand column metric.
[e]DI_{all} is the Deformation Index taking into account all interactions (stacking, Watson-Crick, and non-Watson-Crick).
[f]INF_{all} is the Interaction Network Fidelity taking into account all interactions.
[g]INF_{wc} is the Interaction Network Fidelity taking into account only Watson-Crick interactions.
[h]INF_{nwc} is the Interaction Network Fidelity taking into account only non-Watson-Crick interactions.
[i]INF_{stack} is the Interaction Network Fidelity taking into account only stacking interactions.
[j]Clash Score as computed by the MolProbity suite (Davis et al. 2007).
[k]Significance of the predicted model, assuming that base-pairing was input as a structural constraint (Hajdin et al. 2010).

the *RNA-Puzzles* experiment was taken as an opportunity for training in the use of various modeling methods, in a spirit very similar to the collective work of that group during the CASP5 modeling season (Kosinski et al. 2003). Consequently, a large fraction of human time involved discussions and communication between the two parts of the team physically located in two different cities (Poznan and Warsaw). The human time devoted to interactions with software (preparation of input files, setting up simulations, analyses of output files, and manual refinement

using the graphical user interfaces of SCULPT and HyperChem) was ~30 h, with the majority of time devoted to Problems 2 and 3.

Chen group

The Chen group used a multi-scale approach to predict the RNA 3D structure from the sequence (Cao and Chen 2011). For a given RNA sequence, they first predict the 2D structure from the free

TABLE 4. Pairwise interdomain Deformation Profile values for the helical domains P1, P2, P3, P3a, and P3b from Puzzle 3

	P1xP2	P1xP3	P1xP3a	P1xP3b	P2xP3	P2xP3a	P2xP3b	P3xP3a	P3xP3b	P3axP3b
3_bujnicki_1.dat	19.8	22.5	37.6	46.2	**7.0**	22.2	41.2	**11.2**	27.2	17.7
3_bujnicki_2.dat	27.3	37.3	49.4	68.2	20.1	32.3	47.4	**8.1**	21.5	16.0
3_chen_1.dat	**11.3**	**8.7**	26.0	28.3	**5.1**	18.6	26.8	**12.0**	**14.6**	**14.8**
3_das_1.dat	31.7	36.6	48.9	71.2	18.3	35.6	65.1	**11.9**	30.1	18.9
3_das_2.dat	30.7	32.9	34.1	34.0	24.9	32.9	27.0	**10.4**	**12.6**	**13.4**
3_das_3.dat	29.9	33.7	43.9	59.1	23.2	35.9	45.1	**13.3**	21.9	**13.5**
3_das_4.dat	33.1	36.5	54.0	71.3	**13.1**	22.9	37.9	**9.1**	**13.6**	**10.8**
3_das_5.dat	30.4	34.2	39.1	45.6	25.9	35.1	43.4	**8.9**	**13.5**	**11.8**
3_dokholyan_1.dat	34.9	21.5	32.9	59.4	**12.1**	28.3	32.9	**14.7**	26.8	25.9
3_dokholyan_2.dat	29.0	16.8	21.2	45.5	**13.8**	24.8	35.0	**10.1**	20.9	23.8
3_major_1.dat	23.0	40.3	44.4	46.4	27.5	43.3	56.5	27.9	53.4	48.2
3_major_2.dat	27.6	26.8	44.2	66.1	**9.6**	25.1	37.9	**10.4**	19.4	18.5

All DP values <15 are in boldface.

TABLE 5. The RMSD values for the ligand binding site of each predicted model from Puzzle 3, relative to the crystal structure

	Problem 3
3_das_5	2.842888
3_das_4	2.928573
3_bujnicki_2	3.042605
3_chen_1	3.703777
3_das_2	3.915769
3_dokholyan_2	4.138209
3_bujnicki_1	4.253633
3_major_2	4.447882
3_das_1	4.554707
3_das_3	4.681876
3_dokholyan_1	5.821877
3_major_1	17.289223

energy landscape using the Vfold model (Cao and Chen 2005, 2006a,b, 2009; Chen 2008). The Vfold model allows for the computation of the free energies for the different RNA secondary structures and pseudoknotted structures, from which the (low-free energy) folds can be predicted. Distinguished from other existing models, the Vfold model is based on a virtual bond (coarse-grained) structural model that enables direct evaluation of the entropy parameters for different RNA motifs, including pseudoknotted structures.

The Vfold-based approach to the evaluation of the entropy and the free energy may lead to more reliable 2D structure prediction. For the calculation of 2D structures, the base-stacking energies are adopted from the Turner energy rules (Serra et al. 1994). For the loops, the model enumerates all the possible intraloop mismatched base stacks and evaluates the free energy for each structure. Intraloop base stacks cause large entropic decrease. The parameters for such entropic decrease can be estimated by a theory such as the Vfold model. Next, a 3D coarse-grained scaffold is constructed, based on the predicted 2D structure. In the coarse-grained structure, three atoms (P, C_4, N_1 or N_9) are used to represent each nucleotide. To construct a 3D scaffold, the predicted helix stems are modeled by A-form helices. For the loops/junctions, 3D fragments from the known PDB database were used. Specifically, a structural template database was built by classifying the structures according to the different motifs such as hairpin loops and internal/bulge loops, three-way junctions, four-way junctions, pseudoknots, etc. Then the optimal structural templates for the predicted loops/junctions were searched from the structural template database. The structural templates may partly account for the tertiary contacts ignored in the 2D structure prediction. Third, the Chen group build the all-atom model from the coarse-grained scaffold by adding the bases to the virtual bond backbone. In the final step, they refine the all-atom structure by using AMBER energy minimization. Two thousand steps of minimization were run, applying 500.0 kcal/mol restraints to all the residues, followed by another 2000 steps of minimization without restraints. The final structure after minimization is the one submitted for evaluation in the structure prediction test.

In summary, the computation involves two steps: (a) the prediction of the 2D structure and the construction of the coarse-grained 3D structure and (b) AMBER energy minimization. The computer times (Ta, Tb) for the two steps are (<1 min,

53 min), (<1 min, 81 min), and (26 min, 143 min), for the predictions of the dimer, the square, and the riboswitch domain, respectively. The first step calculation was performed on a desktop PC with Intel Core 2 Duo CPU E8400 at 3.00 GHz, and the second step computation was performed on a Dell EM64T cluster (Intel Xeon 5150 at 2.66 GHz).

For predicting the dimer and the riboswitch structure (Problems 1 and 3), the Chen group only relied on the sequence information, and the 3D structures were generated by computer, with no human interference in the process. For the prediction of the square structure (Problem 2), they used the experimentally determined structure for one strand to refine the other strand. The loops and the secondary structure of the square were computer-predicted using the Vfold model (Cao and Chen 2011).

Das group

The Das group used a newly developed ab initio method called <u>stepwise assembly</u> (SWA) for recursively constructing atomic-detail biomolecular structures in small building steps. Each step involved enumerating several million conformations for each monomer, and all step-by-step build-up paths were covered in polynomial computational time. The method is implemented in Rosetta and uses the physically realistic, Rosetta all-atom energy function (Das and Baker 2008; Das et al. 2010). The Das group has recently benchmarked SWA on small RNA loop-modeling problems (Sripakdeevong et al. 2011). They also applied de novo fragment assembly with full-atom refinement (FARFAR, also implemented in Rosetta), but did not submit those solutions because they either agreed with the SWA models (Problem 1; parts of Problems 2 and 3) or did not give converged solutions (other parts of Problems 2 and 3) (Das et al. 2010).

Due to the deterministic and enumerative nature of SWA, the computational expense is high relative to stochastic and knowledge-based methods. The computational expense ranged from 20,000 (Problem 1) to 50,000 CPU-hours (Problems 2 and 3). Also, because the code was developed "on-the-fly," there was no time to fully optimize the run-time, which is being done now.

The SWA modeling runs were fully automated. Manual input was used near the beginning to set up the runs, and near the end to ensure that models presented a diversity of base-pairing patterns—both of these steps could be easily automated, but the Stepwise Assembly method was still under development during the course of this community-wide, blind RNA prediction experiment.

The lessons learned from the three models are the following.

Problem 1

SWA models 1 and 3 (out of five submitted) performed reasonably well on the 46-nt homodimer, especially at the 9-nt L1 region (see Fig. 1C). Both models correctly predicted the noncanonical *cis* WC/WC C9–C37 base pair and the extrahelical bulge at U39. This accuracy was aided by a strategy that gave entropic bonuses to bulged nucleotides that make no other interactions; the bulges are "virtualized" within Rosetta (Sripakdeevong et al. 2011). In this L1 region, both models gave 1.0 Å all-heavy-atom RMSD to the crystallographic model, excluding the U39 extrahelical bulge. In contrast, none of the five SWA models achieved atomic accuracy in the sequence-identical 9-nt L2 loop (see Fig. 1D; >3.0 Å RMSD). Model 3 did correctly predict C14 to be an

extrahelical bulge and C15 and C32 to be base-paired. However, the exact geometry of the predicted C15–C32 base pair and an additional U16–G31 base pair were incorrect. In the crystallographic model, the base of U16 bulged out and its phosphate formed hydrogen-bonding interactions with the base of G31; in the Das group implementation at the time, they ''virtualized'' the phosphates of any bulged nucleotides along with their bases. Partial virtualization of bulged bases and more rigorous modeling of conformational entropy are under investigation.

Problem 2

The SWA models performed well in the regions of the 100-nt ''self-assembling RNA square'' within putatively regular secondary structure. The Das group did not assume these to be ideal A-form helices but modeled them from scratch. These regions are composed mainly of Watson-Crick base pairs but also included a noncanonical *cis* WC/WC base pair at corner E/F (see Fig. 2C) that SWA model 1 correctly predicted. In contrast, the SWA models did not reach atomic accuracy for any of the 5-nt loops at each of the four corners of the square RNA. This was partly expected because the ''corners'' of the nanosquare originated from a 5-nt bulge in HCV IRES domain IIa (PDB number: 2PN4) (Zhao et al. 2008), which happened to be part of our comprehensive SWA benchmark (Sripakdeevong et al. 2011). There, it was possible to sample the crystallographic loop conformation but not to select it as the lowest-energy structure; the loop forms direct hydrogen bonds to metal ions, and these interactions are not yet modeled in Rosetta.

With this result in mind, after the nanosquare crystal structure was released, it was compared with the full ensemble of models generated by SWA. Loops in corners C/D and G/H were engaged in significant crystal contacts; but loops A/B and E/F should have been amenable to high-accuracy modeling. Indeed, for both of these loops, SWA sampled the crystallographic conformation of these loop regions with a <1.0 Å RMSD, but these models had significantly worse Rosetta energy than the submitted ones. Again, these corners (and indeed all four corners) involved the binding of either divalent metal ions or cobalt hexamine (III). The lesson learned (or verified) from this puzzle is that approximations in the Rosetta all-atom energy function, especially with regard to metal ions, still remain too inaccurate to permit atomic-resolution RNA modeling on a consistent basis. This puzzle has inspired us to develop approaches to include metal ions during the de novo buildup of models.

Problem 3

The Das group's recent research has focused on the prediction of high-resolution motifs as stepping stones to modeling larger RNAs. This glycine riboswitch puzzle was thus currently out of range—its core three-way junction and glycine binding site form an intricate noncanonical pairing network involving more than a dozen residues. Furthermore, interactions across a dimer interface appear crucial for stabilizing the riboswitch conformation, but this information was not available. The group's models were based on generating low-energy Rosetta SWA models for individual loops, two-way junctions, and three-way junctions, and then connecting them with ideal helices. Surprisingly, this basic approach, ignorant of higher-order interactions, gave the best base-pair recoveries (INF all, INF wc, INF nwc; see Models 1 and 2 in Table 3) among submitted models. Other submitted models (Models 4 and 5) gave the best RMSDs for the glycine-binding

site. However, these were very far from atomic accuracy (2.8 Å and 2.9 Å). Most critically, the global structure of the RNA was not recapitulated (RMSD and DI) (Table 3). The helices formed the correct tuning-fork-like rearrangement but were twisted relative to the crystallographic model (Tables 4, 5). Globally correct solutions require global optimization, and this puzzle has motivated the group to develop iterative hybrid high-resolution/low-resolution approaches to RNA modeling, analogous to the rebuild-and-refine method used in Rosetta template-based modeling (Qian et al. 2007). As a final note, in the article describing this puzzle's crystal structure, a striking structural similarity of the glycine riboswitch core to a previously solved SAM-I riboswitch (Montange and Batey 2006) was noted. If such similarities could be inferred from sequence or multiple sequence alignments (analogous to fold recognition methods in protein modeling), we expect that substantially more accurate models could be built. We are therefore hopeful about further development of RNA structural bioinformatics approaches such as Rmdetect (Cruz and Westhof 2011) and FR3D (Sarver et al. 2008).

Dokholyan group

The Dokholyan group adopted a multi-scale, molecular dynamics approach (Ding and Dokholyan 2012). Briefly, coarse-grained discrete molecular dynamics (DMD) simulations are used to sample the vast conformational space of RNA molecules. The representative structures are selected from the coarse-grained simulations based on energies and/or additional filters such as the radius of gyration or other experimentally known parameters. RNA nucleotides are represented in coarse-grained simulations by three pseudo-atoms corresponding to the base, sugar, and phosphate groups (Ding et al. 2008b). The neighboring beads along the sequence are constrained to reflect RNA chain connectivity and local geometry, including covalent bonds, bond angles, and dihedral angles. The parameters for bonded interactions are derived from high-resolution RNA structures. Nonbonded interactions include base-pairing, base-stacking, short-range phosphate–phosphate repulsion, and hydrophobic interactions. These interaction parameters are derived from the sequence-dependent free energy parameters of the individual nearest-neighbor hydrogen bond model (INN-HB) (Mathews et al. 1999). Given an initial coarse-grained RNA model, the corresponding all-atom model is reconstructed and further optimized with all-atom DMD simulations (data not shown). The all-atom DMD RNA modeling approach is an extension of all-atom DMD protein modeling (Ding et al. 2008b). In DMD simulations, the structural information of a given RNA, such as base pairs and distances between specific nucleotides, can be incorporated as constraints to guide RNA folding (Gherghe et al. 2009; Lavender et al. 2010).

The CPU time for DMD simulations depends on RNA length. For the coarse-grained simulations, previous benchmarks suggested a near-linear dependence on RNA length (Ding et al. 2008a). For example, for an RNA of $\sim$80 nt (such as Puzzle 3), the total computational time for the coarse-grained DMD simulation is $\sim$12 h. The procedure to identify representative structures using the clustering algorithm usually requires <1 h. The CPU time of the all-atom DMD simulation also depends on RNA length n, with the computational complexity of order $\sim n \ln(n)$. For the 84-nt RNA (Problem 3), the CPU time was $\sim$18 h; and the CPU time for 100-nt RNA (Problem 2) was $\sim$24 h.

In the current three RNA puzzles, base pairs derived either from previous knowledge (input from the experimentalists in Puzzle 2; RNA secondary structure prediction combined with biochemical validation in Puzzle 3) or from biochemical intuition (Puzzle 1) were included. Once the structural information is gathered and prepared for the refinement simulations, the computational effort is then fully automated.

The Dokholyan group's DMD approach has been designed for fold refinement of relatively large RNAs with complex 3D architectures. It was especially successful with Puzzle 3, where the models recapitulated the global fold well. In an independent structure-prediction exercise, the Dokholyan group also recently predicted a structure for the pseudoknot domain of the hepatitis C virus internal ribosome entry site (Lavender et al. 2010). The structure of a closely related RNA construct was subsequently determined by crystallography (Berry et al. 2011). Their prediction for the HCV pseudoknot domain shows good agreement with the global fold of the experimental structure (RMSD $\approx$ 11 Å and *P*-value 5×10^{-3}), although some local interactions were missed.

For the simpler RNAs in Puzzles 1 and 2, the learned lesson is that inclusion of as much experimentally validated structural information as possible improves predictions, but it is important to avoid over-constraining the simulation. Instead, the DMD simulations should be allowed to sample the favorable conformational space, where constraints are unclear. For example, in their solution to Puzzle 1, the Dokholyan group overestimated the internal base-pairing in the middle of the monomer sequence based on misinterpreting the statement in the puzzle that ''The strands hybridize with blunt ends (C–G closing base pairs).'' As a result, their prediction for Puzzle 1 had the highest RMSD among the predictions. In a post priori simulation, in which only the G–C pairs at the ends were constrained to form base pairs, the predicted model structure had a much smaller RMSD (4.3 Å) and would have ranked among the top third of models.

Flores group

For 3D structure prediction, the Flores group used RNABuilder (named MMB in a subsequent release), an internal coordinate-mechanics code that allows the user to specify the flexibility, forces, constraints, and full or partial structural coordinates to model the structure and/or dynamics of an RNA molecule (Flores and Altman 2010; Flores et al. 2011). Working in internal coordinates has the advantage that regions of known structure in a model can be rigidified, thus eliminating the cost associated with solving the equations of motion for internal rearrangements of that region (Flores and Altman 2011). Steric exclusion can be accounted for economically using collision-detecting spheres that are applied to a subset of atoms in user-specified residues. Any canonical or noncanonical base-pairing interaction catalogued in Leontis et al. (2002), plus stacking and a ''Superimpose'' threading force can be enforced between any and all pairs of residues specified by the user. These features have been used for RNA threading (Flores et al. 2010) and for generating an all-atoms trajectory of ribosomal hybridization using structural and biochemical information (Flores and Altman 2011).

The processing time on a single core of a 3.0 GHz Intel processor was ~94 min. Notice that this run was not optimized for speed, and also that a newer version of RNABuilder (named MMB) is at least twice as fast due to improvements in the underlying Simbody internal coordinate dynamics engine (Sherman et al. 2011).

RNABuilder is intended to be easy to use, and this goal is supported by the use of a single, free-format command file that is prepared using a relatively intuitive syntax comprising terms recognizable by any biologist. However, the package is also designed to provide the user control over the flexibility, forces, and parameters of the model, in order to be useful for a wide variety of applications; hence, it is not automated. The human time required for preparing a run is thus dependent on the experience of the user and the complexity of the task. RNA-Builder is designed to enable fast runtimes; most tasks undertaken require minutes to hours, depending on the task. A trained user can also reduce the degrees of freedom and structure the problem to allow larger integration time steps for greater efficiency. Also, most users in practice will do multiple calculations before coming to a biological conclusion. In this group's experience, the human/computer time ratio is typically much greater than unity.

Major group

This CASP-like contest was an opportunity for the Major group to test their fully automated MC-Fold and MC-Sym pipeline (Parisien and Major 2008). Two students in the laboratory, Véronique Lisi (PhD student in molecular biology) and Marc-Frédérick Blanchet (PhD student in computer science), who did not participate in the development of the pipeline were selected to participate. Lisi solved the Homodimer and Square problems, and Blanchet solved the Riboswitch Domain problem. Except for the Riboswitch Domain, no human intervention or numerical refinement was applied to the structures that were submitted to the contest, or in other words, the structures that were submitted were taken directly from the output of the MC-Sym program. This explains their high Clash Scores.

Homodimer

Lisi concatenated two copies of the given sequence into one that was submitted to MC-Fold using the default parameters, i.e., not considering pseudoknots; best 20 structures; and, explored the best 15% suboptimal structures. The structure predicted with the highest probability (i.e., minimum free energy) was then submitted to MC-Sym. The first 3D structure generated by MC-Sym was submitted to the contest (atomic clashes 1.5 Å all-atoms but hydrogens; backtrack probabilist, width limit 25%, height limit 33%; backbone method estimate, threshold 2.0 Å; maximum of 1000 models, CPU time limit 180 min, seed 3210, RMSD min 3.0 Å side chain only).

Square

Lisi directly used the 2D structure provided as the input to MC-Sym. The first structure generated by MC-Sym was submitted to the contest (using the same parameters as for the Homodimer).

Riboswitch domain

Maria Abella, a MSc student in bioinformatics, suspected that this sequence was a riboswitch. She checked its matching DNA sequence in GenBank and determined that it was from *Vibrio*

cholerae. Then, using BLAST, she found that the sequence was ~100 bp away from the sodium/glycine symporter GlyP gene in *Bacillus subtilis*, which was previously reported to be controlled by a riboswitch (Mandal et al. 2004). The sequence of the *B. subtilis* riboswitch is the same except for one nucleotide as that for Problem 3. Its 2D structure supported by chemical probing data was also published by Mandal et al. (2004).

Suspecting the riboswitch, Blanchet decided to submit two structures. He first predicted 2D structures using MC-Fold (not considering pseudoknots; best 1000 structures; explore the best 15% suboptimal structures). Generating the set of 1000 suboptimal structures took <2 min on an Intel i7 @ 2.67 GHz. He noted that the 2D structure published by Mandal et al. (2004) was absent in the set. He grouped the 1000 structures according to their topologies. Among the topologies, he kept a cloverleaf (four-way junction; the most frequent with 796 structures among the 1000) and a Y-shape (three-way junction), which corresponded to the same topology of the structure published by Mandal et al. (2004). However, the base-pairing pattern of the predicted structure differed much from that published. He then generated decoys of 3D structures using MC-Sym for the best-scoring 2D structure in each chosen topology (atomic clashes 1.5 Å all-atoms but hydrogens; backtrack probabilist, width limit 25%, height limit 33%; backbone method ccm, pucker = C3′-endo, threshold 2.0 Å; maximum of 9999 models, CPU time limit 12 h, seed 3210, RMSD min 1.0 Å side chain only). He edited the MC-Sym input scripts to explore independently and more of the conformational space of each stem in the same allowed time. The structures of the individual stems were merged in complete structures for an additional 12 h. For each topology (5685 Y-shape and 9999 cloverleaf structures), Blanchet selected the centroid model of the 20 best scoring models (according to the P-Score described at the MC-Sym command page; the centroid structure had a P-Score of −61.44). A "Relieve" minimization (see the MC-Sym command page) was applied to both selected models. This operation corrects the major steric conflicts in the backbone but does not refine the overall structure. This is reflected by the high Clash Score in the submitted models.

Lesson for the Major group

Obviously, in Problem 3, the minimum free energy structure predicted by MC-Fold differs from that of the crystal. Worst, it is not even predicted among the 1000 suboptimals. Just for P3, the 2D structure corresponding to the crystal is evaluated at −39.7 kcal/mol (minimum free energy structure for P3 = −47.9 kcal/mol) and ranks near 50th only. It is not possible to see at this time how this structure could be selected by the program unless more information than the sequence is provided. It would be interesting to see the precision of 3D structures that would have been generated by MC-Sym, given that the crystal 2D structure could have been selected. Thus, a decoy of 3D structures using an input script was generated from the correct 2D dot-bracket (from Fig. 3A without the G29:C83:A11 triple), and after applying the "Relieve" minimization, the structures ranged between 7 and 21 Å of RMSD with the crystal structure (data not shown) (best RMSD = 6.8 Å; P-Score = −25.38). However, selecting this best RMSD structure using our P-Scores is not possible, because the best P-Score structure, −53.84, has an RMSD of 10.3 Å with the crystal structure.

SantaLucia group

The SantaLucia group submitted models for Problems 1 and 2. Both models were generated using the de novo modeling module within the RNA123 software suite (Sijenyi et al. 2012). Below is a brief description of the methodology.

Problem 1

The first step was to predict the secondary structure of the submitted sequence. To accomplish this, the sequence 5′-CCGCC GCGCCAUGCCUGUGGCGGUUCGCCGCCGCGCCAUGCCUG UGGCGG-3′ was submitted to a secondary structure–folding algorithm. The UUCG hairpin was added in order to make a continuous chain of RNA, because RNA123 folds a single chain of RNA. The UUCG hairpin was later manually removed once the tertiary structure was predicted. The secondary structure was predicted using a thermodynamics-based dynamic programming algorithm within RNA123 that produced 10 optimal and suboptimal secondary structure folds. A tertiary structure model was computed only for the optimal secondary structures by decomposing the secondary structure into constituent motifs such as internal loops, helices, and hairpins. The 3D structure was then assembled using a motif library. The motif library was generated from RNA structures previously deposited in the PDB (Protein Data Bank). The selection and assembly of the motifs are automated within the RNA123 via an algorithm called BUILDER (Sijenyi et al. 2012), which uses an energy function to score and assemble the 3D model. The manual effort in performing the prediction for Problem 1 was minor, notably in removing the UUCG hairpin after the models were generated.

Comments

After the results for the prediction of Problem 1 were released, the group discovered that they had submitted a model generated from the wrong sequence. Specifically, residue 15 was a C instead of a U, and residue 18 was a U instead of a C. This meant that the dimer ended up with four incorrect residues and thereby compromised the quality of their prediction. It is important to note that this error was later fixed and produced a model that scores better against the crystal structure.

Problem 2

This problem was solved by a combined effort of both manual and automated steps. The given secondary structure was decomposed into four identical "L"-shaped secondary structures with daggling ends on the 5′ end (CCGG) and 3′ end (GGCC). The idea was to generate four identical tertiary structures and then base-pair the daggling ends so that a perfect square (Fig. 2A) can be assembled from the four "L"-shaped structures. Using the de novo modeling module in RNA123, a 3D model with the lowest energy was computed. Fortunately, this model happened to have an "L"-shaped tertiary structure. Four copies of this structure were then created and superimposed onto the provided coordinates of the inner strand from Problem 3, forming an initial coarse model consistent with the "square" secondary structure. This coarse model had distorted base pairs between the 5′ and 3′ dangling ends of each of the preceding fragments, and therefore we subjected

the entire model to the energy optimization algorithm in RNA123. This algorithm, named DSTA (Discrete Sampling of Torsion Angles), uses a multi-dimensional search and a novel method for modeling the local potential energy surface and finding an analytical minimum (Sijenyi et al. 2012).

An estimate of the time required to produce the models

The computer calculation time (on a laptop with Intel Core 2 Duo CPU P8600 @ 2.4 GHz processor) was as follows:

Problem 1. It took ∼25 min to predict a single tertiary structure using the de novo prediction platform in RNA123.

Problem 2. It took ∼20 min to predict and generate four "L"-shaped tertiary structures using the de novo prediction platform in RNA123. Manual assembly and running of the DSTA optimization algorithm took ∼1 h.

An estimate of the proportion human effort/machine effort

Problem 1. Twenty-five minutes of machine effort, negligible human effort.

Problem 2. Twenty minutes of machine effort, 1 h of human effort.

PDB file normalization

Both files for the accepted experimental structures and predicted model files, submitted in PDB format, were normalized to comply with a common standard. Only the first model present in the file was considered. All records except for the ATOM and TER records were ignored. Only the four nucleotides A, C, U, and G were considered. Modified nucleotides were treated as unmodified bases, and extra atoms were discarded (e.g., a 5-bromouracil is treated as a normal uracil and the extra bromine atom is discarded). The only atoms kept are those for the bases (C2, C4, C6, C8, N1, N2, N3, N4, N6, N7, N9, O2, O4, and O6) and for the sugar-phosphate backbone (C1′, C2′, C3′, C4′, C5′, O2′, O3′, O4′, O5′, OP1, OP2, and P).

Stereochemical evaluation

The stereochemical evaluation was performed using the MolProbity (Davis et al. 2007) tool. In a first step, hydrogen atoms were added to the model using the "reduce-build" command line utility, and the Clash Score value was computed using the "oneline-analysis -nocbeta -norota -norama" command.

RMSD computation

The RMSD is computed using the "Superimposer" class from the "Bio.PDB" package (Hamelryck 2003). The "Superimposer" class translates and rotates the comparing model to minimize its RMSD in respect to the reference model. It uses a singular value decomposition algorithm as described in Golub and Van Loan (1989).

Deformation Index and Deformation Profile computations

The base–base interactions (BBI) of both solution and predicted models are extracted using the MC-Annotate (Gendron et al. 2001) tool. The Interaction Network Fidelity (INF) value is computed as:

$$INF = \sqrt{\left(\frac{TP}{TP+FP}\right) \times \left(\frac{TP}{TP+FN}\right)},$$

where TP is the number of correctly predicted BBI, FP is the number of predicted BBI with no correspondence in the solution model, and FN is the number of BBI in the solution model not present in the predicted model. The Deformation Index is then computed as:

$$DI = \frac{RMSD}{INF}.$$

Several partial INF (and respective DI) can be computed if one considers only the Watson-Crick (WC) base pairs (INF_{WC}), the non-Watson-Crick (NWC) base pairs (INF_{NWC}), both WC and NWC base pairs (INF_{BPS}), or the stacking interactions (INF_{STACK}).

The Deformation Profile is a distance matrix computed as the average RMSD between the individual bases of the predicted and the reference models while superimposing each nucleotide of the predicted model over the corresponding nucleotide of the reference model one at a time. It is computed using the "dp.py" command from the "SIMINDEX" package (Parisien et al. 2009).

P-value computation

The *P*-value is computed as described (Hajdin et al. 2010) using:

$$P - value = \frac{1 + erf\left(\frac{(RMSD - <RMSD>)/1.8}{\sqrt{2}}\right)}{2}, \text{ with}$$
$$<RMSD> = a \times N^{0.41} - b.$$

the constants a and b depend on whether the secondary structure base-pairing information is provided ($a = 5.1$ and $b = 15.8$) or not ($a = 6.4$ and $b = 12.7$). This metric is only valid for RNAs with true higher-order 3D folds and thus only applies to Problem 3 (with base-pairing as an assumed constraint).

Graphics

Interactive molecular module images in the *RNA-Puzzles* website are produced with Jmol (http://www.jmol.org) and the secondary structures with VARNA (Darty et al. 2009).

REFERENCES

Berman HM, Westbrook J, Feng Z, Gilliland G, Bhat TN, Weissig H, Shindyalov IN, Bourne PE. 2000. The Protein Data Bank. *Nucleic Acids Res* **28:** 235–242.

Berry KE, Waghray S, Mortimer SA, Bai Y, Doudna JA. 2011. Crystal structure of the HCV IRES central domain reveals strategy for start-codon positioning. *Structure* **19:** 1456–1466.

Boniecki M, Rotkiewicz P, Skolnick J, Kolinski A. 2003. Protein fragment reconstruction using various modeling techniques. *J Comput Aided Mol Des* **17:** 725–738.

Cao S, Chen S-J. 2005. Predicting RNA folding thermodynamics with a reduced chain representation model. *RNA* **11:** 1884–1897.

Cao S, Chen S-J. 2006a. Predicting RNA pseudoknot folding thermodynamics. *Nucleic Acids Res* **34:** 2634–2652.

Cao S, Chen S-J. 2006b. Free energy landscapes of RNA/RNA complexes: With applications to snRNA complexes in spliceosomes. *J Mol Biol* **357:** 292–312.

Cao S, Chen S-J. 2009. Predicting structures and stabilities for H-type pseudoknots with interhelix loops. *RNA* **15:** 696–706.

Cao S, Chen S-J. 2011. Physics-based de novo prediction of RNA 3D structures. *J Phys Chem B* **115:** 4216–4226.

Chen S-J. 2008. RNA folding: Conformational statistics, folding kinetics, and ion electrostatics. *Annu Rev Biophys* **37:** 197–214.

Cruz JA, Westhof E. 2011. Sequence-based identification of 3D structural modules in RNA with RMDetect. *Nat Methods* **8:** 513–519.

Darty K, Denise A, Ponty Y. 2009. VARNA: Interactive drawing and editing of the RNA secondary structure. *Bioinformatics* **25:** 1974–1975.

Das R, Baker D. 2008. Macromolecular modeling with rosetta. *Annu Rev Biochem* **77:** 363–382.

Das R, Karanicolas J, Baker D. 2010. Atomic accuracy in predicting and designing noncanonical RNA structure. *Nat Methods* **7:** 291–294.

Davis IW, Leaver-Fay A, Chen VB, Block JN, Kapral GJ, Wang X, Murray LW, Arendall WB III, Snoeyink J, Richardson JS, et al. 2007. MolProbity: All-atom contacts and structure validation for

proteins and nucleic acids. *Nucleic Acids Res* **35:** W375–W383. doi: 10.1093/nar/gkm216.

Dibrov S, McLean J, Hermann T. 2011a. Structure of an RNA dimer of a regulatory element from human thymidylate synthase mRNA. *Acta Crystallogr D Biol Crystallogr* **67:** 97–104.

Dibrov SM, McLean J, Parsons J, Hermann T. 2011b. Self-assembling RNA square. *Proc Natl Acad Sci* **108:** 6405–6408.

Ding F, Dokholyan N. 2012. Multiscale modeling of RNA structure and dynamics. In *RNA 3D structure analysis and prediction* (ed. NB Leontis, E Westhof). Springer-Verlag, Berlin.

Ding F, Tsao D, Nie H, Dokholyan N. 2008a. Ab initio folding of proteins using all-atom discrete molecular dynamics. *Structure* **16:** 1010–1018.

Ding F, Sharma S, Chalasani P, Demidov VV, Broude NE, Dokholyan NV. 2008b. Ab initio RNA folding by discrete molecular dynamics: From structure prediction to folding mechanisms. *RNA* **14:** 1164–1173.

Ditzler MA, Otyepka M, Sponer J, Walter NG. 2010. Molecular dynamics and quantum mechanics of RNA: Conformational and chemical change we can believe in. *Acc Chem Res* **43:** 40–47.

Flores SC, Altman RB. 2010. Turning limited experimental information into 3D models of RNA. *RNA* **16:** 1769–1778.

Flores SC, Altman R. 2011. Structural insights into pre-translocation ribosome motions. *Pacific Symposium on Biocomputing. Pacific Symposium on Biocomputing* 205-11. http://www.ncbi.nlm.nih.gov/pubmed/21121048.

Flores SC, Wan Y, Russell R, Altman RB. 2010. Predicting RNA structure by multiple template homology modeling. *Pacific Symposium on Biocomputing. Pacific Symposium on Biocomputing* 216-27. http://www.pubmedcentral.nih.gov/articlerender.fcgi?artid=2872935&tool=pmcentrez&rendertype=abstract.

Flores SC, Sherman MA, Bruns CM, Eastman P, Altman RB. 2011. Fast flexible modeling of RNA structure using internal coordinates. *IEEE/ACM Trans Comput Biol Bioinformatics* **8:** 1247–1257.

Gardner PP, Daub J, Tate JG, Nawrocki EP, Kolbe DL, Lindgreen S, Wilkinson AC, Finn RD, Griffiths-Jones S, Eddy SR, et al. 2009. Rfam: Updates to the RNA families database. *Nucleic Acids Res* **37:** D136–D140. doi: 10.1093/nar/gkn766.

Gendron P, Lemieux S, Major F. 2001. Quantitative analysis of nucleic acid three-dimensional structures. *J Mol Biol* **308:** 919–936.

Gherghe CM, Leonard CW, Ding F, Dokholyan NV, Weeks KM. 2009. Native-like RNA tertiary structures using a sequence-encoded cleavage agent and refinement by discrete molecular dynamics. *J Am Chem Soc* **131:** 2541–2546.

Golub G, Van Loan C. 1989. *Matrix computations*. Johns Hopkins University Press, Baltimore.

Hajdin CE, Ding F, Dokholyan NV, Weeks KM. 2010. On the significance of an RNA tertiary structure prediction. *RNA* **16:** 1340–1349.

Hamelryck T. 2003. PDB file parser and structure class implemented in Python. *Bioinformatics* **19:** 2308–2310.

Hofacker IL, Fontana W, Stadler PF, Bonhoeffer LS, Tacker M, Schuster P. 1994. Fast folding and comparison of RNA secondary structures. *Monatsh Chem* **125:** 167–188.

Huang L, Serganov A, Patel DJ. 2010. Structural insights into ligand recognition by a sensing domain of the cooperative glycine riboswitch. *Mol Cell* **40:** 774–786.

Jonikas MA, Radmer RJ, Altman RB. 2009. Knowledge-based instantiation of full atomic detail into coarse-grain RNA 3D structural models. *Bioinformatics* **25:** 3259–3266.

Jossinet F, Ludwig TE, Westhof E. 2010. Assemble: An interactive graphical tool to analyze and build RNA architectures at the 2D and 3D levels. *Bioinformatics* **26:** 2057–2059.

Kosinski J, Cymerman IA, Feder M, Kurowski MA, Sasin JM, Bujnicki JM. 2003. A ''FRankenstein's monster'' approach to comparative modeling: Merging the finest fragments of Fold-Recognition models and iterative model refinement aided by 3D structure evaluation. *Proteins* **53:** 369–379.

Lavender CA, Ding F, Dokholyan NV, Weeks KM. 2010. Robust and generic RNA modeling using inferred constraints: A structure for the hepatitis C virus IRES pseudoknot domain. *Biochemistry* **49:** 4931–4933.

Leontis NB, Westhof E. 2001. Geometric nomenclature and classification of RNA base pairs. *RNA* **7:** 499–512.

Leontis NB, Stombaugh J, Westhof E. 2002. The non-Watson-Crick base pairs and their associated isostericity matrices. *Nucleic Acids Res* **30:** 3497–3531.

Mandal M, Lee M, Barrick JE, Weinberg Z, Emilsson GM, Ruzzo WL, Breaker RR. 2004. A glycine-dependent riboswitch that uses cooperative binding to control gene expression. *Science* **306:** 275–279.

Martinez HM, Maizel JV, Shapiro B. 2008. RNA2D3D: A program for generating, viewing, and comparing 3-dimensional models of RNA. *J Biomol Struct Dyn* **25:** 669–683.

Marti-Renom MA, Madhusudhan MS, Fiser A, Rost B, Sali A. 2002. Reliability of assessment of protein structure prediction methods. *Structure* **10:** 435–440.

Mathews DH, Sabina J, Zuker M, Turner DH. 1999. Expanded sequence dependence of thermodynamic parameters improves prediction of RNA secondary structure. *J Mol Biol* **288:** 911–940.

Matthews B. 1975. Comparison of the predicted and observed secondary structure of T4 phage lysozyme. *Biochim Biophys Acta* **405:** 442–451.

Metropolis N, Ulam S. 1949. The Monte Carlo method. *J Am Stat Assoc* **44:** 335–341.

Michel F, Westhof E. 1990. Modelling of the three-dimensional architecture of group I catalytic introns based on comparative sequence analysis. *J Mol Biol* **216:** 585–610.

Montange RK, Batey RT. 2006. Structure of the *S*-adenosylmethionine riboswitch regulatory mRNA element. *Nature* **441:** 1172–1175.

Moult J. 2006. Rigorous performance evaluation in protein structure modelling and implications for computational biology. *Philos Trans R Soc Lond B Biol Sci* **361:** 453–458.

Murray LJW, Arendall WB, Richardson DC, Richardson JS. 2003. RNA backbone is rotameric. *Proc Natl Acad Sci* **100:** 13904–13909.

Parisien M, Major F. 2008. The MC-Fold and MC-Sym pipeline infers RNA structure from sequence data. *Nature* **452:** 51–55.

Parisien M, Cruz JA, Westhof E, Major F. 2009. New metrics for comparing and assessing discrepancies between RNA 3D structures and models. *RNA* **15:** 1875–1885.

Qian B, Raman S, Das R, Bradley P, McCoy AJ, Read RJ, Baker D. 2007. High-resolution structure prediction and the crystallographic phase problem. *Nature* **450:** 259–264.

Reuter JS, Mathews DH. 2010. RNAstructure: Software for RNA secondary structure prediction and analysis. *BMC Bioinformatics* **11:** 129. doi: 10.1186/1471-2105-11-129.

Rother K, Rother M, Boniecki M, Puton T, Bujnicki JM. 2011a. RNA and protein 3D structure modeling: Similarities and differences. *J Mol Model* **17:** 2325–2336.

Rother M, Rother K, Puton T, Bujnicki JM. 2011b. ModeRNA: A tool for comparative modeling of RNA 3D structure. *Nucleic Acids Res* **39:** 4007–4022.

Rother K, Rother M, Boniecki M, Puton T, Tomala K, Lukasz P, Bujnicki JM. 2012. Template-based and template-free modeling of RNA 3D structure: Inspirations from protein structure modeling. In *RNA 3D structure analysis and prediction* (ed. NB Leontis, E Westhof). Springer-Verlag, Berlin.

Sarver M, Zirbel CL, Stombaugh J, Mokdad A, Leontis NB. 2008. FR3D: Finding local and composite recurrent structural motifs in RNA 3D structures. *J Math Biol* **56:** 215–252.

Serra MJ, Axenson TJ, Turner DH. 1994. A model for the stabilities of RNA hairpins based on a study of the sequence dependence of stability for hairpins of six nucleotides. *Biochemistry* **33:** 14289–14296.

Sherman Ma, Seth A, Delp SL. 2011. Simbody: Multibody dynamics for biomedical research. *Procedia IUTAM* **2:** 241–261.

Sijenyi F, Saro P, Ouyang Z, Damm-Ganamet K, Wood M, Jiang J, SantaLucia J Jr. 2012. The RNA folding problems: Different levels of RNA structure prediction. In *RNA 3D structure analysis and prediction* (ed. NB Leontis, E Westhof). Springer-Verlag, Berlin.

Sripakdeevong P, Kladwang W, Das R. 2011. An enumerative stepwise ansatz enables atomic-accuracy RNA loop modeling. *Proc Natl Acad Sci* **108:** 20573–20578.

Surles MC, Richardson JS, Richardson DC, Brooks FP. 1994. Sculpting proteins interactively: Continual energy minimization embedded in a graphical modeling system. *Protein Sci* **3:** 198–210.

Tinoco I Jr, Bustamante C. 1999. How RNA folds. *J Mol Biol* **293:** 271–281.

Tinoco I Jr, Borer PN, Dengler B, Levin MD, Uhlenbeck OC, Crothers DM, Bralla J. 1973. Improved estimation of secondary structure in ribonucleic acids. *Nat New Biol* **246:** 40–41.

Woese CR, Magrum LJ, Gupta R, Siegel RB, Stahl DA, Kop J, Crawford N, Brosius J, Gutell R, Hogan JJ, et al. 1980. Secondary structure model for bacterial 16S ribosomal RNA: Phylogenetic, enzymatic and chemical evidence. *Nucleic Acids Res* **8:** 2275–2293.

Word JM, Lovell SC, LaBean TH, Taylor HC, Zalis ME, Presley BK, Richardson JS, Richardson DC. 1999. Visualizing and quantifying molecular goodness-of-fit: Small-probe contact dots with explicit hydrogen atoms. *J Mol Biol* **285:** 1711–1733.

Yang H, Jossinet F, Leontis N, Chen L, Westbrook J, Berman H, Westhof E. 2003. Tools for the automatic identification and classification of RNA base pairs. *Nucleic Acids Res* **31:** 3450–3460.

Zemla A. 2003. LGA: A method for finding 3D similarities in protein structures. *Nucleic Acids Res* **31:** 3370–3374.

Zhang Y, Skolnick J. 2004. Scoring function for automated assessment of protein structure template quality. *Proteins* **57:** 702–710.

Zhao Q, Han Q, Kissinger CR, Hermann T, Thompson P. 2008. Structure of hepatitis C virus IRES subdomain IIa. *Acta Crystallogr D Biol Crystallogr* **64:** 436–443.

Zuker M. 2003. Mfold web server for nucleic acid folding and hybridization prediction. *Nucleic Acids Res* **31:** 3406–3415.